Spectral broadening and temporal compression of ∼100 fs pulses in air-filled hollow core capillary fibers

C. Li,[1] K. P. M. Rishad,[1] P. Horak,[2] Y. Matsuura[3] and D. Faccio[1,*]

[1] *School of Engineering and Physical Sciences, SUPA, Heriot-Watt University, Edinburgh EH14 4AS, United Kingdom*

[2] *Optoelectronics Research Centre, University of Southampton, Southampton SO17 1BJ, United Kingdom*

[3] *Graduate School of Biomedical Engineering, Tohoku University, Sendai 980-8579, Japan*

[*] *D.Faccio@hw.ac.uk*

Abstract: We experimentally study the spectral broadening of intense, ∼100 femtosecond laser pulses at 785 nm coupled into different kinds of hollow core capillary fibers, all filled with air at ambient pressure. Differently from observations in other gases, the spectra are broadened with a strong red-shift due to highly efficient intrapulse Raman scattering. Numerical simulations show that such spectra can be explained only by increasing the Raman fraction of the third order nonlinearity close to 100%. Experimentally, these broadened and red-shifted pulses do not generally allow for straightforward compression using, for example, standard chirped mirrors. However, using special hollow fibers that are internally coated with silver and polymer we obtain pulse durations in the sub-20 fs regime with energies up to 300 μJ.

© 2013 Optical Society of America

OCIS codes: (320.5520) Pulse compression; (190.4370) Nonlinear optics, fibers; (190.5530) Pulse propagation and temporal solitons.

References and links

1. J. Cheng, C-S. Liu, S. Shang, D. Liu, W. Perrie, G. Dearden, and K. Watkins, "A review of ultrafast laser materials micromachining," Opt. Laser Technol. **46,** 88–102 (2013).
2. E. A. Gibson, A. Paul, N. Wagner, R. Tobey, D. Gaudiosi, S. Backus, I. P. Christov, A. Aquila, E. M. Gullikson, D. T. Attwood, M. M. Murnane, and H. C. Kapteyn, "Coherent soft X-ray generation in the water window with quasi-phase matching," Science **302,** 95-98 (2003).
3. E. Rubino, J. McLenaghan, S. C. Kehr, F. Belgiorno, D. Townsend, S. Rohr, C. E. Kuklewicz, U. Leonhardt, F. König, and D. Faccio, "Negative-frequency resonant radiation," Phys. Rev. Lett. **108,** 253901 (2012).
4. C. Z. Bisgaard, O. J. Clarkin, G. Wu, A. M. D. Lee, O. Geßner, C. C. Hayden, and A. Stolow, "Time-resolved molecular frame dynamics of fixed-in-space CS_2 molecules," Science **323,** 1464–1468 (2009).
5. K. H. Lee, S. B. Park, H. Singhal, and C. H. Nam, "Ultrafast direct imaging using a single high harmonic burst," Opt. Lett. **38,** 1253–1255 (2013).
6. J. Xia, C. Altucci, S. Amoruso, R. Bruzzese, R. Velotta, and X. Wang, "Generation of high energy, 30 fs pulses at 527 nm by hollow-fiber compression technique," Opt. Express **16,** 3527-3536 (2008).
7. G. Andriukaitis, D. Kartashov, D. Lorenc, A. Pugylys, A. Baltuska, L. Giniunas, R. Danielius, J. Limpert, T. Clausnitzer, E.-B. Kley, A. Voronin, and A. Zheltikov, "Hollow-fiber compression of 6 mJ pulses from a continuous-wave diode-pumped single-stage Yb,Na:CaF_2 chirped pulse amplifier," Opt. Lett. **36,** 1914–1916 (2011).
8. F. M. Mitschke and L.F. Mollenauer, "Discovery of the soliton self-frequency shift," Opt. Lett. **11**, 659-661 (1986)

9. P. Hölzer, W. Chang, J. C. Travers, A. Nazarkin, J. Nold, N. Y. Joly, M. F. Saleh, F. Biancalana, and P. St. J. Russell, "Femtosecond nonlinear fiber optics in the ionization regime," Phys. Rev. Lett. **107**, 203901 (2011).
10. A. Couairon and A. Mysyrowicz, "Femtosecond filamentation in transparent media," Phys. Rep. **441**, 47-189 (2007).
11. M. Nisoli, S. De Silvestri, O. Svelto, R. Szipöcs, K. Ferencz, Ch. Spielmann, S. Sartania, and F. Krausz, "Compression of high-energy laser pulses below 5 fs," Opt. Lett. **22**, 522-524 (1997).
12. D. Faccio, A. Grun, P.K. Bates, O. Chalus, and J. Biegert, "Optical amplification in the near-infrared in gas-filled hollow-core fibers," Opt. Lett. **34**, 2918-2920 (2009).
13. S. Varma, Y.-H. Chen, and H. M. Milchberg, "Trapping and destruction of long-range high-intensity optical filaments by molecular quantum wakes in air," Phys. Rev. Lett. **101,** 205001 (2008).
14. B. E. Schmidt, W. Unrau, A. Mirabal, S. Li, M. Krenz, L. Wöste, and T. Siebert, "Poor man's source for sub 7 fs: a simple route to ultrashort laser pulses and their full characterization," Opt. Express **16,** 18910-18921 (2008).
15. Y. Matsuura, M. Miyagi, K. Shihoyama, and M. Kawachi, "Delivery of femtosecond pulses by flexible hollow fibers," J. Appl. Phys. **91,** 887–889 (2002).
16. G.P. Agrawal, "Effect of intrapulse stimulated Raman scattering on soliton-effect pulse compression in optical fibers," Opt. Lett. **15,** 224-226 (1990).
17. P. Horak and F. Poletti, "Multimode nonlinear fibre optics: theory and applications," in *Recent Progress in Optical Fiber Research*, M. Yasin, S. W. Harun, and H. Arof, eds. (Intech, 2012), pp. 3-25.
18. R. T. Chapman, T. J. Butcher, P. Horak, F. Poletti, J. G. Frey, and W. S. Brocklesby, "Modal effects on pump-pulse propagation in an Ar-filled capillary," Opt. Express **18**, 13279-13284 (2010).
19. T. J. Butcher, P. N. Anderson, R. T. Chapman, P. Horak, J. G. Frey, and W. S. Brocklesby, "Bright extreme-ultraviolet high-order-harmonic radiation from optimized pulse compression in short hollow waveguides," Phys. Rev. A **87**, 043822 (2013).
20. J. R. Peñano, P. Sprangle, B. Hafizi, A. Ting, D. F. Gordon, and C. A. Kapetanakos, "Propagation of ultra-short, intense laser pulses in air," Phys. Plasmas **11**, 2865-2874 (2004).
21. http://refractiveindex.info/?group=GASES&material=Air
22. G. Khanarian and Hoechst Celanese, "Optical properties of cyclic olefin copolymers," Opt. Eng. **40,** 1024–1029 (2001).

1. Introduction

Ultrafast lasers have many applications, such as micromachining [1], nonlinear optics [2, 3], ultrafast spectroscopy [4], direct imaging [5], etc. Different approaches to generating ultrafast laser sources with shorter pulse durations, higher pulse energy, and in different wavelength regimes may be adopted. One of the most common and successful approaches for the compression of fs pulses with milli-Joule energies is to use hollow core fibers filled with gas, typically Argon at a pressure optimized in order to achieve efficient spectral broadening via self phase modulation (SPM), albeit with a sufficiently flat phase that may be efficiently compensated for externally, e.g. by dielectric mirrors with tailored dispersion. These techniques have been widely demonstrated and utilized with relatively short (40 fs or less) input pulses. However, far less attention has been devoted to applying this technique to longer pulses, e.g. in the $\sim$100 fs regime. Notable exceptions are recent results with 300 fs pulses at 527 nm [6] and 200 fs at 1030 nm, compressed to 20-30 fs in capillaries filled with noble gases [7].

The first and crucial step to pulse compression in these fibers is of course the spectral broadening. In the absence of any higher order effects, SPM alone will symmetrically broaden the pulse spectrum around the input carrier frequency. Dispersion terms higher than the second order will unbalance the energy content. Major distortions of the spectral broadening will occur in the presence of delayed nonlinearities related for example to the Raman response or laser pulse induced plasma. The Raman effect is well known to produce a strong red-shift when the pulse is propagating in the negative group velocity (GVD) dispersion regime. This is usually referred to as intrapulse Raman scattering and is readily observed in solitons propagating in solid core fibers [8]. Recently, a new regime has been uncovered in which solitons or pulses propagating in the negative GVD regime in noble gas filled hollow core fibers undergo a strong blue shift [9]. In this case, plasma is generated by the pulse and leads to a decreasing refractive index on the pulse trailing edge that blue shifts the pulse. This effect is also well known

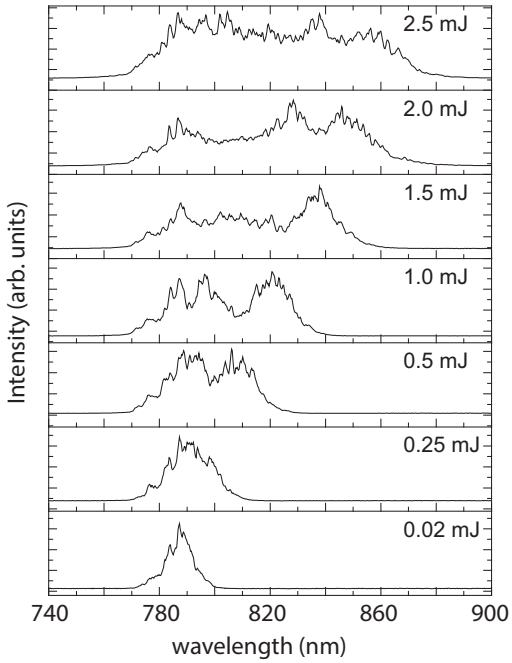

Fig. 1. Experimentally measured spectra with different input pulse energies from the 700 μm core fiber with internal silver and polymer coating (fiber E). The transform limited pulse duration of these spectra vs. input pulse energy is 78, 56, 36, 28, 21, 20, 19 fs for 0.02, 0.25, 0.5, 1.0, 1.5, 2.0, 2.5 mJ input energy. All fibers investigated delivered very similar spectra.

in the normal GVD regime in both bulk and large diameter hollow core fibers used for high energy (mJ or higher) pulse compression (see e.g. [10–12]). Conversely, spectral red-shifting is typically not observed in positive GVD: in solid core fibers the pulse will usually temporally broaden and thus reduce the peak intensity before efficient red-shifting can take place. In hollow core fibers mostly noble gases are used that do not exhibit delayed Raman nonlinearities. Even if air is used as a nonlinear medium, short pulse lengths of typically $\sim$30-50 fs pulses are input into the fiber and thus the Raman nonlinearity remains largely ineffective. Indeed, it has been shown that the Raman nonlinearity of air only starts to play a role when the input pulse duration is of the order of 100 fs or more [13].

Here we are motivated by the possibility of compressing high energy (1-2 mJ) pulses with $\sim$ 100 fs duration under the simplest possible conditions, along the same lines of reasoning as the "poor man's approach to ultrashort pulses" [14]. We therefore investigate $\sim$100 fs pulse compression based on spectral broadening in capillaries filled simply with air at ambient pressure and subsequent re-compression with a set of chirped mirrors that provide a defined amount of second order dispersion per bounce. This approach greatly simplifies the experimental realization as it does not require any vacuum or gas chambers. We primarily investigate the pulse spectral broadening in ambient pressure air and we uncover the important role played by the Raman nonlinearity in this regime that in our experiments appears to completely dominate the pulse evolution. Our findings are supported by numerical simulations that confirm the dominant role of the Raman effect at these pulse durations. Our experimental results also show that a standard, glass capillary does not lead to readily compressible pulses. Conversely, capillaries

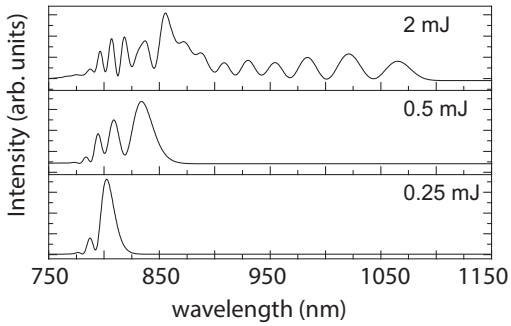

Fig. 2. Numerically simulated spectra with different input pulse energies from the 700 μm core fiber with internal silver and polymer coating (fiber E) assuming 100% Raman contribution to the nonlinearity.

with an internal coating of silver and polymer do allow post compression down to sub-20 fs durations with standard, commercially available chirped mirrors.

2. Experiments

The laser is an amplified Ti:Sapphire femtosecond laser from Amplitude Technologies (90 fs, 100 Hz, 12 mJ/pulse). Pulses with energies varying from 0.1 to 3 mJ are coupled into various hollow core fibers (also often called capillary fibers, i.e. they are simple tubes of glass). Some of the fibers are internally coated with silver in order to reduce propagation losses. For some fibers there is an additional polymer layer deposited on top of the silver coating. The original scope of this polymer layer was to further improve the transmission characteristics although we found that it may also modify the fiber dispersion. The parameters of the fibers are as follows:
- Fiber A: 1 meter long, 200 μm inner core diameter, 350 μm outer core diameter, uncoated silica fiber.
- Fiber B: 1 meter long, 700 μm inner core diameter, 850 μm outer core diameter, uncoated silica fiber.
- Fiber C: 1 meter long, 300 μm inner core diameter, 750 μm outer core diameter, internally silver-coated silica fiber (silver coating is less than 1 μm).
- Fiber D: 0.8 meter long, 320 μm inner core diameter silica fiber, 450 μm outer core diameter, internally coated with silver (300 nm) and polymer (350 nm) [15].
- Fiber E: 1 meter long, 700 μm inner core diameter silica fiber, 850 μm outer core diameter, internally coated with silver (300 nm) and polymer (350 nm).

The fibers are placed on a precisely machined aluminium V-groove to ensure its straightness and left at ambient air pressure. The two ends of the aluminium V-groove are precisely aligned by two 3 dimensional translation stages. Laser light is coupled into the fibers by focusing with lenses chosen such that a 60% fill factor is obtained. By careful alignment, we can get a sharp intensity peak at the output, which will be selected with an iris for further pulse compression using chirped mirrors. In general, the hollow core fiber with bigger core size will have higher transmission efficiency. For hollow core fibers with the same core size, the fiber with silver coating inside will have higher transmission efficiency, because the silver coating will increase the reflection efficiency of the light at high input angle. However, the actual transmission losses do not vary too much with fiber diameter: all uncoated fibers exhibited a total transmission loss of $\sim$60% and were very sensitive to alignment. All coated fibers exhibited transmission losses of the order of 20-30% and were less susceptible (in the losses) to alignment errors. The output

spectra are measured using a standard fiber-coupled spectrometer.
Figure 1 shows an example of the spectral broadening obtained at the output of fiber E. The total transmission efficiency, accounting for waveguide losses, ionization and all other effects, for this fiber is ∼80%. The spectra are broadened yet a clear red-shift is observed. We note that this red-shift with practically identical features was observed with all of our fibers. It is therefore not due to the specific coating or characteristics of the fiber and should be ascribed to the nonlinearity of air. If only self-phase modulation, i.e. the instantaneous component of the nonlinearity were present, we would expect to see the spectrum broaden symmetrically to both sides of the central laser wavelength, or possibly exhibit a typical blue shift associated with pulse self-steepening and plasma formation that occurs at the higher input energies. On the contrary, the evident spectral red-shift is a clear indication of the dominant role of the Raman nonlinearity, in agreement with previous studies that also show that for pulses in the ∼100 fs regime, Raman (i.e. the molecular rotational nonlinearity) dominates [13]. However, this red-shift is remarkable in that, whereas intrapulse Raman scattering is known to red-shift solitons [16], similar effects have not been observed before in media with normal group velocity dispersion (GVD).

3. Numerical simulations

In order to verify these conclusions and ascertain the role of the Raman nonlinearity, we performed a series of numerical simulations. These simulations are based on a multimode generalized nonlinear Schrödinger equation [17] that accounts for mode dispersion, nonlinear Kerr and Raman effects, self-steepening, ionization, plasma refractive index, and nonlinear mode coupling, which has been tested previously for high-power pulse propagation in short capillaries [18, 19]. The lowest 15 transverse modes with rotational symmetry were included in the simulations (for details of mode calculations and sample dispersion curves see Sec. 4 below) and the launch was assumed to be by Gaussian pulses into the fundamental mode. The nonlinearity of air was modeled as by J. R. Peñano et al. in [20], but the fractional contribution of the Raman effect to the full nonlinearity was used as an additional free parameter. In Fig. 2 we show the simulated output spectra for the same case (fiber E) as Fig. 1 and assuming 100% Raman contribution. We observe a qualitatively good agreement between the spectra; most importantly, we capture the increasing red-shift with increasing input power with no blue-shifted part of the spectrum. In the numerical simulations this red-shift appears to be somewhat more extended than in the experiment (e.g. at 2 mJ a long spectral tail extending out to 1.2 μm wavelength is observed). This difference could possibly be due to deviations of the pulse shape from the ideal Gaussian in the experiment, partial launch into higher order modes, and the lower sensitivity of the silicon detector-based spectrometer above 900 nm. We underline that in order to achieve this agreement it was necessary to increase the Raman fraction up to 100%. Anything short of this produced also blue-shifted components and at 50% Raman fraction the unbalance between red and blue shifted components is nearly negligible (data not shown). This therefore highlights that already for input pulse durations $\sim$ 100 fs, third order nonlinear effects in air are completely dominated by the Raman response.

4. Pulse compression

We now present the results concerning the actual pulse temporal compression, starting from the two uncoated glass fibers, A and B.
The temporal profiles are characterized using a frequency-resolved optical gating (FROG) setup and FROG traces at different input energies are recorded. For fiber A, without any post-compression chirped mirrors, when we increase the input energy the pulse duration first increases but then drops to about 75 fs that illustrated in Fig. 3(a). We attribute this behavior to

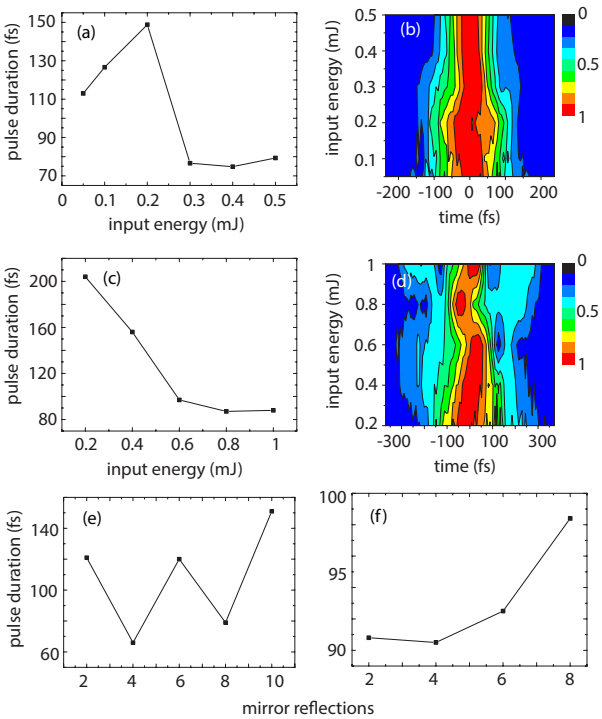

Fig. 3. (a) Pulse duration versus input energy for fiber A. (b) Reconstructed time profiles for fiber A at different input energies. (c) Pulse duration versus input energy for fiber B. (d) Reconstructed time profiles for fiber B at different input energies. (e) Pulse duration at different number of bounces on the chirped mirrors for fiber B. (f) Pulse duration at different number of bounces on the chirped mirrors for fiber C.

possible "soliton-like" dynamics related to the fact that the GVD for fiber A is (weakly) negative around 800 nm. Fiber B on the other hand has a larger core diameter and the GVD for the fundamental mode around 800 nm is positive, so we expect the pulse duration to follow significantly different dynamics, as shown in Fig. 3(c). Although the pulse duration measured at the FWHM appears to decrease continuously, we note that the full temporal profile shown in Fig. 3(d) exhibits strong wings that are an indication of strong self-modulation effects in normal GVD. We then fixed the input energy at 1 mJ, and we attempted to compress the pulses using a pair of GDD-oscillation compensated chirped mirrors (Layertec) in order to compensate the positive group dispersion delay (GDD) from the fiber, self-phase modulation and other processes. The chirped mirrors have high reflection between 540 and 1040nm (manufacturer specifications), much broader than the spectra that we generated, so it will reflect the whole spectra and nothing is truncated. We have indeed verified that there is no spectral reshaping occurring on the mirrors. The compression is due solely to the dispersion introduced by the mirrors. Every two bounces (one bounce on each mirror) on these chirped mirrors give a negative GDD of -40$\pm$20fs^2. As can be seen in Fig. 3(e), the FWHM of the pulse never decreases below 60 fs even if the spectrum should support transform-limited pulses with durations below 20 fs. Very similar results, shown in Fig. 3(e) were obtained also with fiber C that has an internal silver coating.

As a short conclusion, we found that spectral broadening in air-filled capillaries followed by standard chirped mirrors with negative GDD is not a viable route for efficient pulse compres-

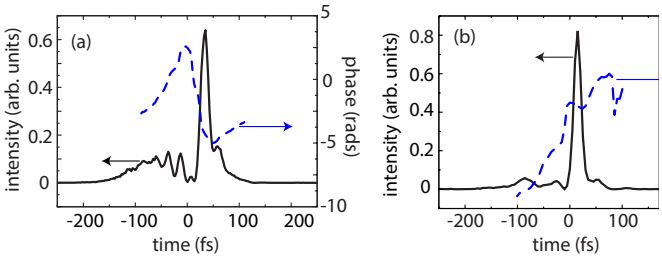

Fig. 4. (a) Reconstructed time profile for fiber D (recompressed with 6 mirror bounces). (b) Reconstructed time profile for fiber E (recompressed with 8 mirror bounces).

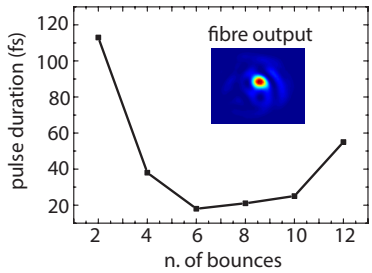

Fig. 5. Pulse durations for fiber D with varying number of bounces on two chirped mirrors.

sion. We believe that this is due to the dominant role of the Raman nonlinearity that, we must conclude, gives efficient spectral broadening albeit with a spectral phase that does not allow compression by simple techniques.

However, the situation is somewhat different with fibers D and E: these two fibers are inner coated with 300 nm silver plus an additional 350 nm polymer layer [15]. Figure 4(a) illustrates the reconstructed temporal profile from fiber D that shows a main sharp peak with a wide yet significantly weaker (less than 15%) pedestal, after re-compression with 6 bounces on the mirrors. Figure 5 illustrates the pulse duration with even number of bounces on the two chirped mirrors varying from 2 to 12, showing that indeed at 6 bounces the pulse duration is minimized. Fiber E is 20 cm longer than fiber D and also has a larger ($\sim 2\times$) core diameter yet we obtain similar or even better results and the larger core diameter allows us to couple higher input energies. The input energy is 2.5 mJ and by adjusting the alignment it is possible to (repeatedly) isolate an output profile with a strong peak which has 10% of the input energy and can be isolated with the help of a pin hole, which is illustrated in the inset in Fig. 5. Figure 4(b) shows the reconstructed temporal profile with a pulse duration of 16 fs from fiber E. We note that this pulse also exhibits a much improved visibility with a pedestal intensity less than 5% of the pulse peak. The overall efficiency is 40% for fiber D and 10% for fiber E. We underline that these "overall" efficiencies refer to the transmitted energy after the iris that is used at the fiber output to select the bright central spot. The reason why the hollow fiber with bigger core size has lower overall efficiency is that the output from the bigger core hollow fiber is highly multimode and a lot of energy is lost to the surrounding background of the output spatial mode.

An interesting question is of course why the polymer coated fibers allow efficient pulse compression whilst other fibers do not. A first evaluation seems to clearly indicate that the polymer modifies the fiber dispersion properties significantly. We calculate the effective refractive indices (n_{eff}) of different modes using a commercial software (Lumerical) for the 1st and 3rd

output modes of fiber D. The refractive indices of SiO_2 and silver at different wavelengths are from the database of the software (MODE Solutions). The refractive index of air is calculated by using the dispersion formula [21]. The polymer used in these fibers is a cyclic olefin polymer that is taken with a constant refractive index value n = 1.53 in the spectral range of interest here [22]. From the theoretical calculations, we see that the polymer coating does not change the spatial mode evolution, but it changes the dispersion properties of the hollow core fiber, therefore it changes the phase of the output beam and makes it compressible. We underline that the dispersion of the gas inside the fiber is very weak. It therefore requires only a very slight modification of the fiber parameters to create a large effect in relative terms to the overall dispersion. Indeed, this is what happens: The mode overlap with the polymer is not large or significant but nevertheless sufficient to change the weak waveguide and gas dispersion properties. Figure 6 shows the 2nd and 3rd order dispersions for the first and third modes of fiber D, compared to the same fiber without the polymer coating. Clearly the coating is strongly

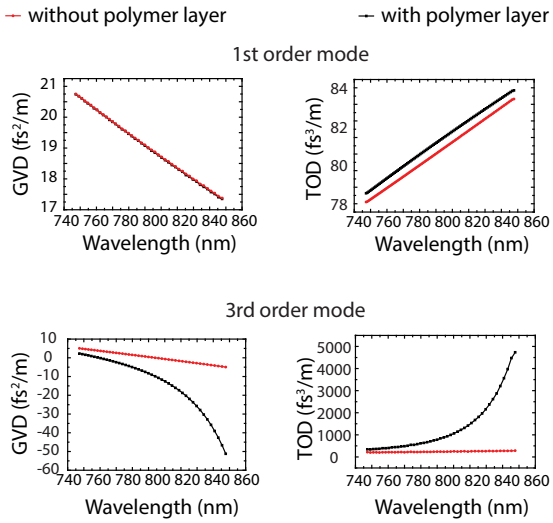

Fig. 6. GVD and TOD of the hollow core fiber with and without polymer coating for the 1st and 3rd order output mode.

modifying the dispersion. This is due to a sharp resonance at around 900 nm where the hollow core modes couple strongly to a bound mode of the thin polymer layer. For higher order modes (not shown) the influence of the polymer increases to the point that it could indeed start to significantly modify the pulse dispersion during propagation, thus indicating a possible role in the pulse compression. Unfortunately full NLSE simulations as described in Sec. 3 were not able to capture this effect. We believe that this may be due to the prohibitively large number of modes that would be required in the numerics in order to faithfully reproduce not only the intensity but also the phase dynamics of the pulse propagation. Future work will be devoted to investigating these aspects.

5. Conclusions

We have demonstrated efficient pulse spectral broadening in ambient pressure, air-filled capillaries of $\sim$ 100 fs Ti:Sapph pulses with temporal compression down to 16 fs, using a pair of dispersion-compensating mirrors, and output energies up to 300 μJ in a smooth, Gaussian-shaped spatial mode. At these input pulse durations the Raman nonlinearity leads to very strong

intrapulse scattering and red-shifting. This is in stark contrast to the expected and usually observed blue-shifted continuum generated by SPM in noble gases and also hints to the possible utilization of Raman and delayed nonlinearities as an additional method for ultrashort laser pulse control.

Acknowledgments

D.F. acknowledges financial support from the European Research Council under the European Union's Seventh Framework Programme (FP/2007-2013)/ERC GA 306559 and EPSRC (UK, Grant EP/J00443X/1).